# Optimal Attitude Control for Articulated Body Mobile Robots

**Edwardo F. Fukushima** *and* **Shigeo Hirose**

Tokyo Institute of Technology, Dept. of Mechano-Aerospace Engineering,
2-12-1 Ookayama, Meguro-ku, Tokyo 152-8552, Japan
fukusima@mes.titech.ac.jp *and* hirose@mes.titech.ac.jp

**Abstract**

Optimal force distribution has been active field of research for multifingered hand grasping, cooperative manipulators and walking machines. The articulated body mobile robot "KORYU" composed of cylindrical segments linked in series and equipped with many wheels have a different mechanical topology, but it forms many closed kinematic chains through the ground and presents similar characteristics as the above systems. This paper introduces an attitude control scheme for the actual mechanical model "Koryu-II (KR-II)", which consists of optimization of force distribution considering quadratic object functions, combined with attitude control based on computed torque method. The validity of the introduced method is verified by computer simulations and experiments using the actual mechanical model KR-II.

## 1. Introduction

The authors have been developing a new type of mobile robot configuration called an "Articulated Body Mobile Robot". This class of robot has a snake-like configuration and is composed of many segments linked in series. This configuration introduces advantageous characteristics such as high rough terrain adaptability and load capacity, among others. Two mechanical models of articulated body mobile robot called KORYU (KR for short) have been developed and constructed, so far. KORYU was mainly developed for use in fire-fighting reconnaissance and inspection tasks inside nuclear reactors. However, highly terrain adaptive motions can be achieved by KR: 1) stair climbing, 2) passing over obstacles without touching them, 3) passing through meandering and narrow paths, 4) running over uneven terrain, and 5) using the body's degrees of freedom not only for "locomotion", but also for "manipulation". Many other related studies have been reported [3]-[10], but very few practical mechanical implementations are available.

The fundamental control strategies necessary for KORYU to perform the many inherent motion capabilities are: 1) Attitude Control; 2) Steering Control [1]; and 3) Mobile Manipulator Control [2]. This paper in particular address the attitude control problem.

Figure 1: KR-II moving on uneven terrain.

### 1.1. Attitude control problem description

KR-II is composed of cylindrical units (**Fig.2**(a)(b)) linked in series by prismatic joints which generate vertical motion between adjacent segments. These prismatic joints are force controlled so that each segment vertical position automatically adapts to the terrain irregularities, as shown in **Fig.3**(a). The most simple implementation of force control is to make these joints free to slide. However, in this case the system acts like a system of wheeled inverted pendulum carts connected in series and is unstable by nature, as shown in **Fig.3**(b). Thus, an attitude control scheme to maintain the body in the vertical posture is demanded. This work introduces a new attitude control based in optimal force distribution calculation using quadratic programming for minimization of joint energy consumption. As pointed out in detail in this paper, this method shares similarities with force distribution for multifingered hands, multiple coordinated manipulators and legged walking robots.

This paper is organized as follows: In Section 2 the background on optimal force distribution problem is described. Section 3 introduces the optimal force dis-

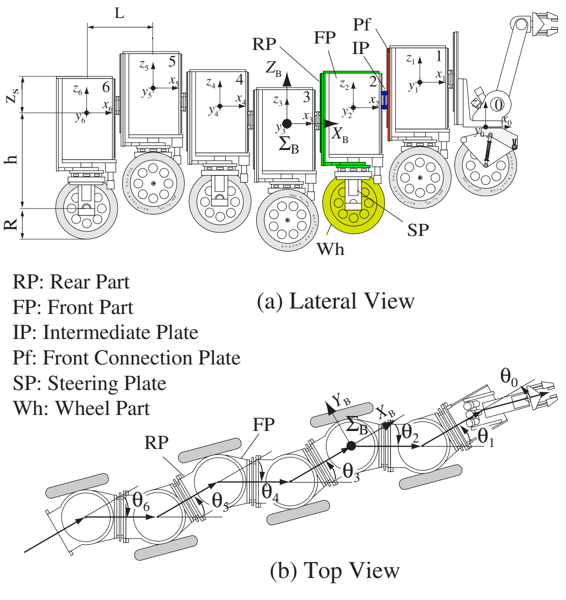


Figure 2: KR-II's mechanism and motion variables.

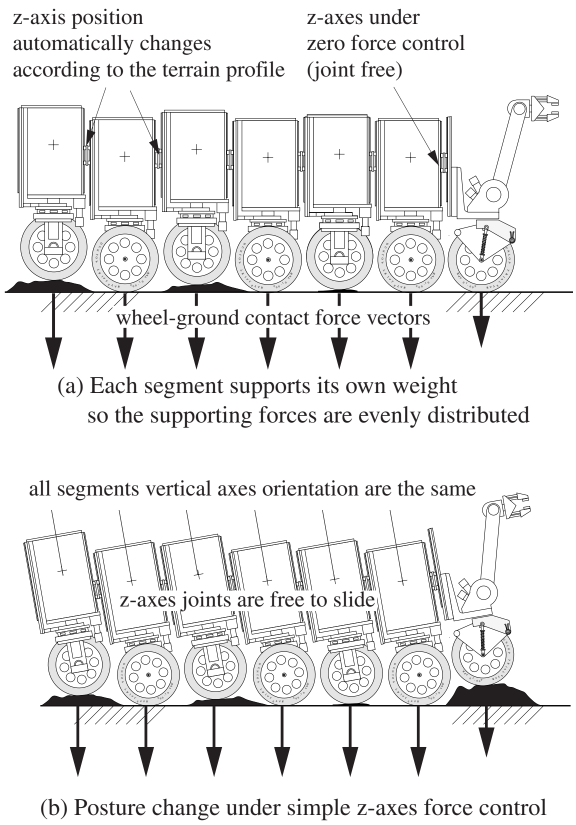


Figure 3: Effects of force control.

tribution formulation and shows an efficient algorithm to solve this problem. Section 4 presents the mechanical modeling of KR-II and introduces the feedback control law for attitude control. Finally in Section 5 the computer simulation and experimental results are shown to demonstrate the validity of the introduced method.

## 2. Background on Optimal Force Distribution Problem

Many types of force distribution problems have been formulated for multifingered hands, multiple coordinated manipulators and legged walking robots. A brief review of the fundamental concepts and similarities with formulation of balance equation and equations of motion of multibody systems are described.

### 2.1. Balance equations for the reference member

Multifingered hands, multiple coordinated manipulators and legged walking robots can be modeled as one *reference member* with $k$ external contact points as shown in **Fig.4**(a). Consider the reference member parameters given by: mass $m_0$; linear and angular acceleration at the center of mass $\boldsymbol{\alpha}_0, \boldsymbol{\omega}_0 \in \boldsymbol{R}^3$; inertia tensor at the center of mass coordinate $\boldsymbol{H}_0 \in \boldsymbol{R}^{3\times3}$; force $\boldsymbol{F}_i \in \boldsymbol{R}^3$and moment $\boldsymbol{M}_i \in \boldsymbol{R}^3$ acting on the $i$th contact point; position of the contact point with respect to the center of mass coordinate $\boldsymbol{p}_i = [\, p_{i1} \quad p_{i2} \quad p_{i3}\,]^T \in \boldsymbol{R}^3$. The resulting force and moment at the center of mass is given by $\boldsymbol{F}_0 = \sum_{i=1}^{k} \boldsymbol{F}_i \in \boldsymbol{R}^3$ and $\boldsymbol{M}_0 = \sum_{i=1}^{k} (\boldsymbol{M}_i + \boldsymbol{p}_i \times \boldsymbol{F}_i) \in \boldsymbol{R}^3$. The balance equations is given below, where the gravitational acceleration $\boldsymbol{g}$ which in principle is an external force, was included in the left term for simplicity of notation.

$$m_0\,(\boldsymbol{\alpha}_0 - \boldsymbol{g}) = \boldsymbol{F}_0 \qquad (1)$$

$$\boldsymbol{H}_0\,\dot{\boldsymbol{\omega}}_0 + \boldsymbol{\omega}_0 \times (\boldsymbol{H}_0\,\boldsymbol{\omega}_0) = \boldsymbol{M}_0 \qquad (2)$$

The inertial terms can be grouped as $\boldsymbol{Q} \in \boldsymbol{R}^6$, and the external force terms into the matrix $\boldsymbol{P}$ and vector of contact points $\boldsymbol{N}$,

$$\boldsymbol{P} = \begin{bmatrix} \boldsymbol{I}_3 & 0 & \cdots & \boldsymbol{I}_3 & 0 \\ \tilde{\boldsymbol{p}}_1 & \boldsymbol{I}_3 & \cdots & \tilde{\boldsymbol{p}}_k & \boldsymbol{I}_3 \end{bmatrix} \in \boldsymbol{R}^{6\times 6k} \qquad (3)$$

$$\tilde{\boldsymbol{p}}_i = \begin{bmatrix} 0 & -p_{i3} & p_{i2} \\ p_{i3} & 0 & -p_{i1} \\ -p_{i2} & p_{i1} & 0 \end{bmatrix} \in \boldsymbol{R}^{3\times3}$$

$\boldsymbol{I}_3 \in \boldsymbol{R}^{3\times3}$ : Identity Matrix

$$\boldsymbol{N} = [\, \boldsymbol{F}_1^T \quad \boldsymbol{M}_1^T \quad \cdots \quad \boldsymbol{F}_k^T \quad \boldsymbol{M}_k^T \,]^T \in \boldsymbol{R}^{6k} \qquad (4)$$

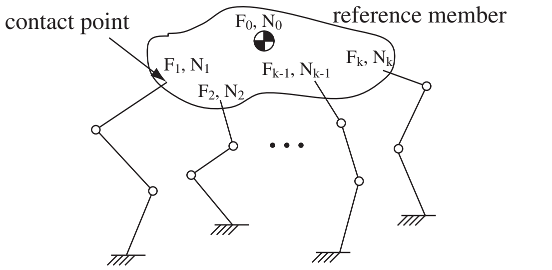


(a) Multifingered hands, multiple coordinated manipulators and legged walking robots

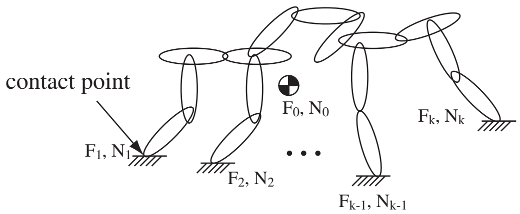


(b) A general multibody system (KR included)

Figure 4: Comparison of single and multibody systems.

Thus the balance equations are described by the following linear relation.

$$\boldsymbol{Q} = \boldsymbol{P}\,\boldsymbol{N} \tag{5}$$

#### 2.1.1. *General solution*

The general solution of Equation (5) with respect to $\boldsymbol{N}$ is given by

$$\boldsymbol{N} = \boldsymbol{P}^{+}\boldsymbol{Q} + (\boldsymbol{I} - \boldsymbol{P}^{+}\boldsymbol{P})\boldsymbol{\lambda} \tag{6}$$

as described in reference [12], where $\boldsymbol{P}^{+}$ is a generalized pseudo-inverse matrix.

Basic formulation of force distribution and description about internal forces concepts were first addressed by Kerr and Roth [11]. The fundamental concepts are: i) the general solution can be divided in two orthogonal vectors $\boldsymbol{N} = \boldsymbol{N}_e + \boldsymbol{N}_i$; ii) the partial solution $\boldsymbol{N}_e$ can be solved by $\boldsymbol{N}_e = \boldsymbol{P}^{+}\boldsymbol{Q}$ using the pseudo-inverse matrix; iii) the partial solution $\boldsymbol{N}_i$ resides in the null-space of $\boldsymbol{P}$ and corresponds to the internal forces; iv) $(\boldsymbol{I} - \boldsymbol{P}^{+}\boldsymbol{P})$ is a matrix formed by orthonormal basis vectors which span the null space of $\boldsymbol{P}$, and $\boldsymbol{\lambda}$ corresponds to the magnitude of the internal forces. Kerr and Roth used these concepts to formulate a linear programming problem which took in account friction forces at contact points and also joint driving forces.

Force distribution problem for gripper and hands usually results in searching optimal values for $\boldsymbol{\lambda}$. Nakamura et al were the first to formulate a nonlinear problem using quadratic cost function $||\boldsymbol{N}||$ to solve the internal forces [13]. Efficient solutions using linear programming were also analyzed by other authors [14][16]. Nahon and Angeles [15] showed that minimization of internal forces and joint torques can both be formulated in an efficient quadratic programming method, and Goldfarb and Idnami method [19] can be used to solve this problem. Other efficient formulations are also been investigated [17][18].

### 2.2. Multibody systems

Multibody systems differ from multifingered hands as shown in **Fig.4**(a)(b) not only by the fact that in general they have no commom reference member, but also because that forces and moments $\boldsymbol{F}_i, \boldsymbol{M}_i$ acting in the contact points arises from different phisical natures. In system (a) the external forces are exerted from the fingers, manipulators or legs. However, system (b) can not have external forces exerted from the ground. Instead, the forces and moments at the contact points are originated from the gravitational acceleration and internal motion of the system itself. However, balance equations and equations of motion for these systems present similar characteristics as described next.

#### 2.2.1. *Balance equations*

Let the variables $k$, $\boldsymbol{F}_i$, $\boldsymbol{M}_i$, $\boldsymbol{p}_i$ be defined the same in **Fig.4**(a)(b), the Equations (3)(4) are valid for both systems, but Equations (1)(2) due to inertial forces are not. However, the total force acting on the systems's center of mass can be derived as $\boldsymbol{Q}(\boldsymbol{q}, \dot{\boldsymbol{q}}, \ddot{\boldsymbol{q}})$, i.e., as function of generalized coordinate $\boldsymbol{q}, \dot{\boldsymbol{q}}, \ddot{\boldsymbol{q}}$. Hence, the balance equations can be described by

$$\boldsymbol{Q}(\boldsymbol{q},\, \dot{\boldsymbol{q}},\, \ddot{\boldsymbol{q}}) = \boldsymbol{P}\,\boldsymbol{N} \tag{7}$$

Equations (7) and (5) are mathematically equivalent, and therefore the fundamental theory discussed in section 2.1.1 can also be applied to multibody systems.

#### 2.2.2. *Equations of motion*

For the system in **Fig.4**(a), the problem of finding optimal values for contact forces $\boldsymbol{N}$ and joint forces $\boldsymbol{\tau}$ can be independently formulated. However, the equations of motion can also be grouped as Equation (8) for optimization of joint forces of the entire system [12].

$$\boldsymbol{\tau} = \boldsymbol{H}\ddot{\boldsymbol{q}} + \boldsymbol{C} + \boldsymbol{G}_g + \boldsymbol{J}^T\boldsymbol{N} \tag{8}$$

It is well known that Equation (8) has the same structure for robot manipulators and multibody-systems where $\boldsymbol{H}$ is the inertial term, $\boldsymbol{C}$ the coriolis and centrifugal term, $\boldsymbol{G}_g$ the gravitational term, and $\boldsymbol{J}$ is the Jacobian matrix. Therefore, the equations of motion for systems in **Fig.4**(a) and (b) are mathematically equivalent.

# 3. Efficient Algorithm for Solving Optimal Force Distribution Problem

## 3.1. Cost function

Electrical motor's energy consumption at low speed but high output torque operation can be estimated by the power loss in the armature resistance. Hence, the sum of squares of joint forces $\boldsymbol{\tau}$ can be used as the cost function to be minimized.

$$S(\boldsymbol{\tau}) = \boldsymbol{\tau}^T \boldsymbol{W} \boldsymbol{\tau} \tag{9}$$

Note that $\boldsymbol{W}$ is a symmetric positive definite matrix. Now let $\boldsymbol{H}_q = \boldsymbol{H}\ddot{\boldsymbol{q}} + \boldsymbol{C} + \boldsymbol{G}_g$, $\boldsymbol{G} = 2\boldsymbol{J}\boldsymbol{W}\boldsymbol{J}^T$ and $\boldsymbol{d} = 2\boldsymbol{J}\boldsymbol{W}\boldsymbol{H}_q$ be defined as auxiliary variables. Substituting Equation (8) into (9) results in

$$S(\boldsymbol{\tau}) = \boldsymbol{H}_q^T \boldsymbol{W} \boldsymbol{H}_q + \boldsymbol{d}^T \boldsymbol{N} + \frac{1}{2}\boldsymbol{N}^T \boldsymbol{G} \boldsymbol{N} \tag{10}$$

a new cost function depending on the variable $\boldsymbol{N}$.

## 3.2. Quadratic problem formulation

The first term in the right side of Equation (10) does not depend on $\boldsymbol{N}$, so the new const function can be described by Equation (11). A general quadratic programming problem can now be formulated as Equations (11)(12)

$$\underset{\boldsymbol{N}}{min.}: \quad S(\boldsymbol{N}) = \boldsymbol{d}^T \boldsymbol{N} + \frac{1}{2}\boldsymbol{N}^T \boldsymbol{G} \boldsymbol{N} \tag{11}$$

$$\text{subject to:} \begin{cases} \boldsymbol{P}_e \boldsymbol{N} = \boldsymbol{Q}_e \\ \boldsymbol{P}_i \boldsymbol{N} \geq \boldsymbol{Q}_i \end{cases} \tag{12}$$

Equations (12) are linear constraint equations, with equality constraints given by Equations (5) or (7), and inequality constraints given by the system's friction, contact and joint force limitations. A positive definite matrix $\boldsymbol{W}$ guarantees this problem to be strictly convex, thus having efficient solution algorithms [19].

## 3.3. Solution considering equality constraints

The partial problem when considering only equality constraints can be solved as

$$\boldsymbol{N}_e = \boldsymbol{P}_e^+ \boldsymbol{Q}_e - \boldsymbol{H}_e \, \boldsymbol{d} \tag{13}$$

with generalized pseudo-inverse matrix $\boldsymbol{P}_e^+$ defined as

$$\boldsymbol{P}_e^+ = \boldsymbol{G}^{-1} \boldsymbol{P}_e^T (\boldsymbol{P}_e \boldsymbol{G}^{-1} \boldsymbol{P}_e^T)^{-1} \tag{14}$$

and auxiliary matrix $\boldsymbol{H}_e$ defined as

$$\boldsymbol{H}_e = (\boldsymbol{I} - \boldsymbol{P}_e^+ \boldsymbol{P}_e) \boldsymbol{G}^{-1} \tag{15}$$

From the observation that the first term of Equation (13) corresponds to the norm of $\boldsymbol{N}$, i.e., the solution which minimizes $\boldsymbol{N}^T \boldsymbol{G} \boldsymbol{N}$, the second term is the partial solution which minimizes the norm of $\boldsymbol{\tau}$. Note that although it resides in the null-space of $\boldsymbol{P}_e$ an analytic solution is available.

## 3.4. Solution considering inequality constraints

Problems with inequality constraints usually do not have analytical solutions but use some kind of search algorithms [13][15][19]. In order to achieve better real-time performance, only negative contact forces will be considered in this formulation. This is valid for hands, grippers, walking machines and mobile robots in general, that can exert positive forces, i.e., "push", but can not exert negative forces, i.e., "pull". The proposed method introduces a new equality constraints term $\boldsymbol{P}_d \boldsymbol{N} = \boldsymbol{Q}_d \in \boldsymbol{R}^d$ into the balance Equation $\boldsymbol{P}\boldsymbol{N} = \boldsymbol{Q}$,

$$\boldsymbol{P}_e = [\boldsymbol{P}^T \quad \boldsymbol{P}_d^T]^T \tag{16}$$

$$\boldsymbol{Q}_e = [\boldsymbol{Q}^T \quad \boldsymbol{Q}_d^T]^T \tag{17}$$

The basic idea is to transform the problem with inequality constraints into a problem with only equality constraints that can be solved efficiently by Equation (13). This is accomplished by the algorithm described below. Note that the variable $d$ represents the number of contact points included in the equality constraints.

*Step 0.* Initialization: case $d_0 > 0$ make $d = d_0$ and include the contact forces $\boldsymbol{P}_d \boldsymbol{N} = \boldsymbol{Q}_d \in \boldsymbol{R}^{d_0}$ into Equations (16)(17). Case $d_0 = 0$, initialize $\boldsymbol{P}_e = \boldsymbol{P}$ and $\boldsymbol{Q}_e = \boldsymbol{Q}$.

*Step 1.* Calculate the partial solution $\boldsymbol{N}_e$ considering only equality constraints from Equation (13).

*Step 2.* Let the number of negative contact forces in the solution $\boldsymbol{N}_e$ be $d_n$. Case $d_n > 0$ go to *Step 3.* Otherwise, this is the optimal solution. Calculate joint forces by Equation (18). Finish.

$$\boldsymbol{\tau}_e = \boldsymbol{H}_q + \boldsymbol{J}^T \boldsymbol{N}_e \tag{18}$$

*Step 3.* Update $d = d + d_n$. Case $d \leq$ (free variables − balance equations) go to *Step 4*. Otherwise the problem can not be solved. Finish.

*Step 4.* Set the desired contact force at the contact points where resulted in negative forces to zero and include in the equality constraint $\boldsymbol{P}_d\boldsymbol{N} = \boldsymbol{Q}_d$. Return to *Step 1*.

Although this algorithm is suited for real time applications, it does not search for all the combination of possible solutions. For this reason it might finish in *Step 3.* even a possible solution exists. However, for normal steering control, passing-over pipes and ditches, and attitude control of KR-II, a possible solution was always found after a limited number of iterations. An example will be later described in Section 5.

## 4. KR-II's Attitude Control

### 4.1. KR-II's variables

KR-II's motion freedoms can be grouped as: z-axes linear displacements $\boldsymbol{z} = [\, z_1 \quad z_2 \quad \cdots \quad z_6 \,]^T \in \boldsymbol{R}^6$; $\theta$-axes angular displacements $\boldsymbol{\theta} = [\, \theta_0 \quad \theta_1 \quad \cdots \quad \theta_6 \,]^T \in \boldsymbol{R}^7$; wheel's angular displacements $\boldsymbol{s} = [\, s_0 \quad s_1 \quad \cdots \quad s_6 \,]^T \in \boldsymbol{R}^7$; body's coordinate position $\boldsymbol{c}_0 = [\, x_0 \quad y_0 \quad z_0 \,]^T$ and attitude $\boldsymbol{\phi} = [\, \phi_X \quad \phi_Y \quad \phi_Z \,]^T$ relative to the inertial coordinate. This accounts for 26 degrees of freedom. KR-II's inertial parameters are listed in **Table 1**. Note that the extra loads were accounted in the body's front part (FP).

In this work, balance and motion equations given by Equations (7)(8) were derived by Newton-Euler method, but other efficient virtual power methods [7] can also be used.

Table 1: KR-II's inertial parameters.

| Seg | Part | mass [kg] | Inertia[kg m$^2$] | | | mass center [mm] | | |
|---|---|---|---|---|---|---|---|---|
| | | | $I_x$ | $I_y$ | $I_z$ | $p_x$ | $p_y$ | $-p_z$ |
| 0 | FP | 5.0 | 0.04 | 0.04 | 0.01 | 120 | 0 | 300 |
| | SP | 28.0 | 0.24 | 0.24 | 0.07 | 0 | 0 | 570 |
| | RP | 10.8 | 0.40 | 0.30 | 0.08 | -100 | 0 | 270 |
| | Wh | 3.6 | 0.12 | 0.06 | 0.12 | 0 | 0 | 778 |
| 1 | FP | 35.4 | 1.27 | 1.27 | 0.42 | 64 | 9 | 273 |
| 2 | FP | 41.7 | 1.73 | 1.71 | 0.45 | 54 | 17 | 227 |
| 3 | FP | 32.1 | 1.27 | 1.28 | 0.35 | 70 | 0 | 278 |
| 4 | FP | 45.6 | 1.64 | 1.71 | 0.45 | 46 | 17 | 229 |
| 5 | FP | 31.6 | 1.11 | 1.13 | 0.35 | 70 | 0 | 291 |
| 6 | FP | 40.2 | 1.60 | 1.60 | 0.46 | 56 | 0 | 241 |
| 1∼5 | RP | 9.5 | 0.24 | 0.19 | 0.05 | -230 | 0 | 170 |
| 6 | RP | 4.2 | 0.11 | 0.09 | 0.02 | -225 | 0 | 186 |
| 1∼6 | IP | 4.5 | 0.04 | 0.01 | 0.03 | 218 | 0 | 150 |
| | SP | 7.2 | 0.03 | 0.04 | 0.03 | 0 | 80 | 744 |
| | Wh | 3.6 | 0.12 | 0.06 | 0.12 | 0 | 240 | 778 |

(Parts abbreviations)
FP: front part
RP: rear part
IP: intermediate plate
SP: steering plate
Wh: wheel part

(Extra internal loads [kg])
Seg1: extra servo-amp (5.8)
Seg2: on-board computer (12.1)
Seg3: attitude sensor (2.5)
Seg4: battery-pack (16.0)
Seg5: DC-DC converter (2.0)
Seg6: AC-DC converter (10.6)

### 4.2. Simplifications

#### 4.2.1. *Wheel modeling*

The wheel will be simplified to a simple model:

1. It is a thin circular plate with constant radius.
2. It contacts a horizontal plane even when moving on slopes.

However, the horizontal plane is set independently for each wheel so that this simplification is effective for motion over uneven terrains. Nonetheless, for stair climbing and step overcoming motions, a better contact point estimation algorithm is under investigation.

#### 4.2.2. *Other simplifications*

1. **External contact forces:** the wheel's lateral and longitudinal forces are small because optimal trajectory are planned by the steering control [1] and also abrupt acceleration and deceleration are avoided. Moreover, moments between the tire and the ground are also negligible. For these reasons, the tire normal force $F_{z_i}$ can be considered the only external force acting on the system. Hence the external contact force vector is given by

$$\boldsymbol{N} = [\, F_{z0} \quad F_{z1} \quad \cdots \quad F_{z6} \,]^T \in \boldsymbol{R}^7 \qquad (19)$$

2. **Joint forces:** z-axes and $\theta$-axes motions can be independently planned because KR's z-axes orientations are controlled to be always vertical. In fact, $\theta$-axes are position controlled and their desired angular displacements are planned by the steering control [1]. On the other hand, although s-axes motion can be used for the attitude control, it would involve undesirable acceleration and deceleration in the system. For these reasons, z-axes forces will be set as the variables to be optimized.

$$\boldsymbol{\tau} = [\, f_{z0} \quad f_{z1} \quad \cdots \quad f_{z6} \,]^T \in \boldsymbol{R}^7 \qquad (20)$$

Note that $f_{z0}$ was included just for avoiding singularity in the calculation, but always result in $f_{z0} = 0$.

3. **Balance equations:** from the above considerations, force balance in the z direction and moment balance around x and y direction are enough to model our system. Hence, the dimension of the balance Equation $\boldsymbol{P}\,\boldsymbol{N} = \boldsymbol{Q}$ becomes $\boldsymbol{Q} \in \boldsymbol{R}^3$ and $\boldsymbol{P} \in \boldsymbol{R}^{3\times 7}$.

4. **Generalized accelerations:** only a part of the 26 degrees of freedom of KR-II, $\boldsymbol{q}_s = [\,\boldsymbol{z}^T \quad \boldsymbol{\theta}^T \quad \phi_X \quad \phi_Y\,]^T$ and its time derivative $\dot{\boldsymbol{q}}_s = [\,\dot{\boldsymbol{z}}^T \quad \dot{\boldsymbol{\theta}}^T \quad \dot{\phi}_X \quad \dot{\phi}_Y\,]^T$ is used in the calculation. The acceleration variables are further simplified to

$$\ddot{\boldsymbol{q}}_a = [\,\ddot{x}_0 \quad \ddot{y}_0 \quad \ddot{z}_0 \quad \ddot{\phi}_X \quad \ddot{\phi}_Y\,]^T \qquad (21)$$

and used as $\ddot{\boldsymbol{q}} \equiv \ddot{\boldsymbol{q}}_a$.

5. **Other parameters:** other dimensions are as follows: $\boldsymbol{H} \in \boldsymbol{R}^{7\times 5}$; $\boldsymbol{C} \in \boldsymbol{R}^7$; $\boldsymbol{G}_g \in \boldsymbol{R}^7$; $\boldsymbol{J} \in \boldsymbol{R}^{7\times 7}$; $\boldsymbol{P}_d \in \boldsymbol{R}^{d\times 7}$; $\boldsymbol{Q}_d \in \boldsymbol{R}^d$.

### 4.3. Attitude feedback law

The formulation described so far, solves for joint forces which balance the system in a given desired posture. This is fundamentally an inverse dynamics problem. A feedback control law shown below is added into Equation (21)

$$\ddot{\phi}_X = \ddot{\phi}_{X_d} + K_{P_X}(\phi_{X_d} - \phi_{X_m}) - K_{D_X}\dot{\phi}_{X_m} \qquad (22)$$
$$\ddot{\phi}_Y = \ddot{\phi}_{Y_d} + K_{P_Y}(\phi_{Y_d} - \phi_{Y_m}) - K_{D_Y}\dot{\phi}_{Y_m} \qquad (23)$$

where $K_P, K_D$ are proportional and derivative gain and the indexes $d, m$ stands for desired and measured values. This control law is equivalent to the (*Computed Torque Method*)[20] so that the closed-loop system stability can be analyzed in the same way.

## 5. Computer Simulation and Experimental Results

Computer simulation and experiment using the real robot KR-II, were evaluated for an "obstacle passing over (without touching them)" where a box shape obstacle with width 300mm and height 150mm was considered. This motion was performed at a constant forward velocity of 100mm/s. The vertical motion of each segment is shown in **Fig.5**(a). Note that the calculated displacement includes a 10mm displacement for safety, resulting in a 160mm total vertical displacement.

### 5.1. Continuity of calculated forces

Discontinuities in the calculated forces occurs when topological changes are caused by lifting-up or touching-down of the wheels. In this paper these discontinuities are avoided by introducing desired contact forces using the equality constraints $\boldsymbol{P}_d\boldsymbol{N} = \boldsymbol{Q}_d$ in *Step 0*. The desired forces when lifting-up is given as

$$F_{d_n} = F_{Up_n}\frac{(50 - Z_n)}{50} \qquad (24)$$

and when touching-down the ground is given as

$$F_{d_n} = F_{Down_n}\frac{(50 - Z_n)}{50} \qquad (25)$$

$F_{Up_n}$ is the optimal force calculated just before the wheel lift-up, $F_{Down_n}$ is the optimal force calculated considering that the wheel has completely touch-down the ground, $Z_n$ is the segment vertical diplacement as shown in **Fig.5**(a). These equations are applied only in the interval $Z_n = 0 \sim 50$mm. The constant 50 was derived considering KR-II's spring suspension stroke. For vertical displacements above 50, the desired contact force is set to zero. The simulation results shown in **Fig.5**(b)-(c) demonstrate the validity of the proposed method.

### 5.2. Experimental results

The experiment was held applying the feedforward command shown in **Fig.5**(c) and feedback command given by Equations (22) and (23). The feedback gains were $K_{P_X} = 65$, $K_{D_X} = 18$, $K_{P_Y} = 95$, $K_{D_Y} = 16$ and all the computation were performed in real-time with a sampling-time of 20ms using a 486DX2-50MHz CPU based PC. The experiment overview is shown in **Fig.6**.

**Fig.7**(a) shows the performance of attitude control. Large attitude changes occur at times when more than one segment is lifted-up at the same time, but the overall performance is acceptable for finishing the passing-over motion. The sum of squares of z-axes joint forces measured during the experiment is shown in **Fig.7**(b), which has the same tendency as the simulation result in **Fig.5**(d).

## 6. Summary and Conclusions

An attitude control scheme based in optimal force distribution using quadratic programming, which minimize joint energy consumption was derived in this paper. Similarities with force distribution for multifingered hands, multiple coordinated manipulators and

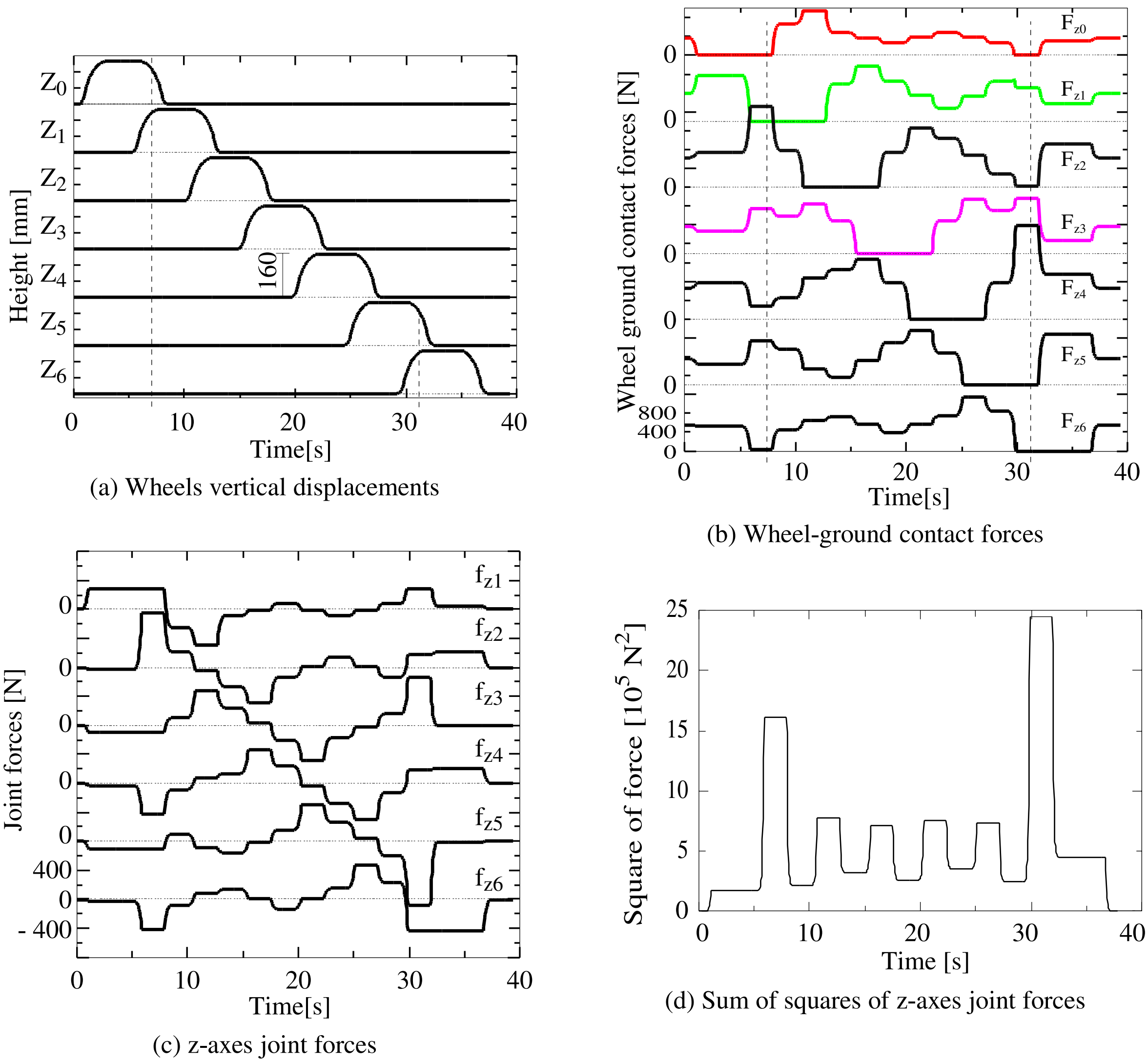


(a) Wheels vertical displacements

(b) Wheel-ground contact forces

(c) z-axes joint forces

(d) Sum of squares of z-axes joint forces

Figure 5: Obstacle passing over simulation.

legged walking robots were demonstrated. The attitude control scheme was introduced inside this force distribution problem, and successfully implemented for control of the articulated body mobile robot KR-II. Validity and effectiveness of proposed methods were verified by computer simulation and also experimentally using the actual mechanical model KR-II.

## References


[1] E. F. Fukushima, S. Hirose, "Efficient Steering Control Formulation for The Articulated Body Mobile Robot "KR-II"," *Autonomous Robots*, Vol. 3, No. 1, pp. 7-18, 1996.

[2] E. F. Fukushima, S. Hirose, and T. Hayashi, "Basic Manipulation Considerations For The Articulated Body Mobile Robot," *Proc. of the 1998 IEEE/RSJ Int. Conf. on Intelligent Robotics and Systems*, pp. 386-393, 1998.

[3] K. J. Waldron, V. Kumar and A. Burkat: "An actively coordinated mobility system for a planetary rover," *Proc. 1987 ICAR*, pp.77-86, 1987.

[4] Commissariat A I'Energie Atomique: "Rapport d'activite 1987," *Unité de Génie Robotique Avancé*, France, 1987.

[5] J. W. Burdick, J. Radford and G. S. Chirikjian: "Hyper-redundant robots: kinematics and experiments," *International Symposium on Robotics Research*, pp.1-16, 1993.

[6] D. Tilbury, O. J. Sordalen and L. Bushnell: "A Multisteering Trailer System: Conversion

Figure 6: Experiment overview.

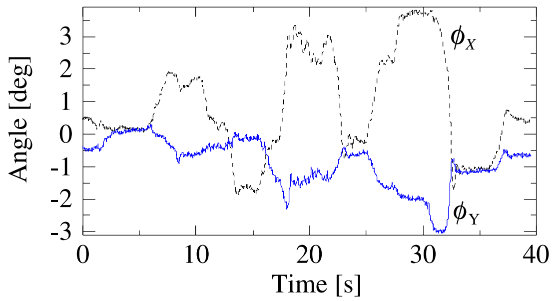


(a) Attitude displacements

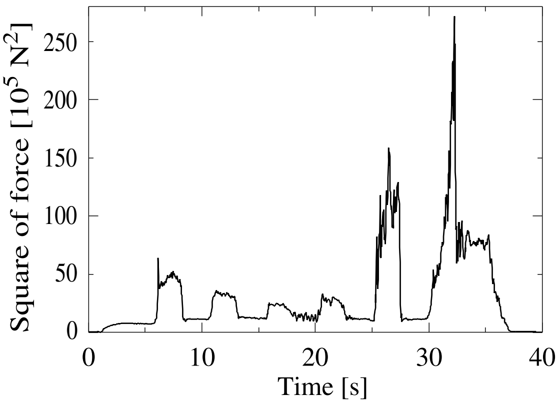


(b) Sum of squares of z-axes joint forces

Figure 7: Obstacle passing over experiment results.


into Chained Form Using Dynamic Feedback," *IEEE Transactions on Robotics and Automation*, Vol.11, No.6, pp.807-818, 1995.

[7] K. Thanjavur and R. Rajagopalan: "Ease of Dynamic Modelling of Wheeled Mobile Robots (WMRS) using Kane's Approach," *Proc. of IEEE Intl. Conference on Robotics and Automation*, pp.2926-2931, 1997.

[8] Y. Shan and Y. Koren: "Design and Motion Planning of a Mechanical Snake," *IEEE Transactions on System, Man and Cybernetics*, Vol.23, No.4, pp.1091-1100, 1993.

[9] Martin Nilsson, "Snake Robot Free Climbing," *Proc. IEEE Intl. Conference on Robotics and Automation*, pp.3415-3420, 1997.

[10] G. Migads and J. Kyriakopoulos, "Design and Forward Kinematic Analysis of a Robotic Snake," *Proc. IEEE Intl. Conference on Robotics and Automation*, pp.3493-3497, 1997.

[11] Jeffrey Kerr and Bernard Roth, "Analysis of Multifingered Hands," *The Intl. Journal of Robotics Research*, Vol.4, No.4, pp.3-17, 1986.

[12] Ian D. Walker, Robert A. Freeman and Steven I. Marcus: "Dynamic Task Distribution for Multiple Cooperating Robot Manipulators," *Proc. IEEE Intl. Conf. on Robotics and Automation*, pp.1288-1290, 1988.

[13] Y. Nakamura, K. Nagai, T. Yoshikawa: "Dynamics and Stability in Coordination of Multiple Robotic Mechanisms," *The Intl. Journal of Robotics Research*, Vol.8, No.2, pp.44-61, 1989.

[14] F. T. Cheng and D. E. Orin, "Optimal Force Distribution in Multiple-Chain Robotic Systems," *IEEE Transactions on Systems, Man, and Cybernetics*, Vol. 21, No.1, pp. 13-24, 1991.

[15] Meyer A. Nahon and Jorge Angeles, "Real-Time Force Optimization in Parallel Kinematic Chains under Inequality Constraints," *IEEE Trans. on Robotics and Automation*, Vol.8, No.4, pp.439-450, Aug. 1992.

[16] M. Buss, H. Hashimoto and J. Moore, "Dextrous Hand Grasping Force Distribution," *IEEE Transactions on Robotics and Automation*, Vol.12, No.3, pp.406-418, 1996.

[17] Jeng-Shi Chen, Fan-Tien Cheng, Kai-Tarng Yang, Fan-Chu Kung and York-Yin Sun, "Solving the Optimal Force Distribution Problem in Multilegged Vehicles," *Proc. of the 1998 IEEE Intl. Conf. on Robotics and Automation*, pp.471-476, Belgium, May 1998.

[18] Duane W. Markefka and David E. Orin, "Quadratic Optimization of Force Distribution in Walking Machines," *Proc. of the 1998 IEEE Intl. Conf. on Robotics and Automation*, pp.477-483, Belgium, May 1998.

[19] D. Goldfarb, A. Idnami, "A numerically stable dual method for solving strictly convex quadratic programs", *Math. Programming*, Vol. 27, pp.1-33, 1983.

[20] B. R. Markiewics, "Analysis of the Computer Torque Drive Method and Comparison with Conventional Position Servo for a Computer-Controlled Manipulator," *Jet Propulsion Laboratory, California Institute of Technology*, TM 33-601, March 1973.